ISSN 1070-3284, Russian Journal of Coordination Chemistry, 2014, Vol. 40, No. 6, pp. 424–431. © Pleiades Publishing, Ltd., 2014.

# Copper(II) and Lead(II) Complexes Based on 2,3,5,6-*tetrakis*(2-Pyridyl)Pyrazine as a Polydentate Ligand[1]

**A. S. Saljooghi[a], *, H. A. Rudbari[b], F. Nicolò[b], A. Salimi[a], F. Delavarmendi[a], and M. Zahmati[a]**

[a] *Department of Chemistry, Ferdowsi University of Mashhad, Mashhad, 91779 Iran*

[b] *Dipartimento di Chimica Inorganica, Chimica Analitica e Chimica Fisica, Università di Messina, Messina, 98166 Italy*

**e-mail: amir.saljooghi@yahoo.com; saljooghi@um.ac.ir*

Recieved April 19, 2012

**Abstract**—The Cu(II) complexes [Cu(Tppz)(Dipic)] · $8H_2O$ (**I**) and $[Pb_2(Tppz)Cl_4]_n$ (**II**), where Tppz, $H_2$Dipic are 2,3,5,6-*tetrakis*(2-pyridyl)pyrazine, dipicolinic acid, respectively, have been synthesized and characterized by elemental analyses, IR, cyclic voltammetry, and electronic spectral studies. Solid state structures of both complexes have been determined by single crystal X-ray crystallography. An ORTEP drawing of two complexes shows that the coordination geometry around the metal center is a distorted octahedron. There are extensive conventional intermolecular O–H···O, N–H···O, and weaker C–H···O and C–H···Cl non-classical hydrogen bonds, which cause the stability of the crystal structure. Crystal data for **I**: monoclinic, space group: $C2/c$, $a = 35.421(3)$, $b = 8.422(6)$, $c = 22.824(8)$ Å, $\beta = 101.69(2)°$, $V = 6668(5)$ Å$^3$, $Z = 8$. Crystal data for **II**: triclinic, space group $P\bar{1}$, $a = 7.9534(4)$, $b = 8.8682(5)$, $c = 9.4245(5)$ Å, $\beta = 95.086(2)°$, $V = 655.93(6)$ Å$^3$, $Z = 2$.

**DOI:** 10.1134/S1070328414060062

## INTRODUCTION

Tridentate ligands offer the possibility of controlling the stereochemistry of octahedral metal complexes. When a symmetric tridentate ligand is coordinated to a metal ion, there is only one possible stereoisomer. If symmetric tridentate bridging ligands are used in the construction of multimetallic systems, there is only one possible isomer for the whole multimetallic system. Furthermore, the whole complex is a linear, rod-like system. This fixes the metal–metal distance which is essential in understanding energy and electron transfer. Tridentate bridged systems therefore offer many advantages over bidentate bridged systems where the metal–metal distance and photophysical properties can vary depending on the coordination of the ligands. Even though tridentate ligands offer advantages in transition metal complexes, there has been less work done with tridentate ligands than with bidentate ligands [1–4].

Many different types of tridentate ligands which act in different coordination modes, have been investigated [5, 6]. 2,3,5,6-*tetrakis*(2-Pyridyl)pyrazine (Tppz) and pyridine-2,6-dicarboxylic acid (known as dipicolinic acid ($H_2$Dipic) are two type of these tridentate ligands.

Tppz was synthesized more than 50 years ago [7]. The molecule has recently attracted interest for its role as a building block in the construction of highly conjugated extended solids. The five heterocyclic rings contain six nitrogen atoms which can act as Lewis bases. Four of these (the pyridyl nitrogens) are very mobile in relation to the other two, leading to a variety of potential coordination modes. A number of researchers have investigated transition metal complexes of Tppz because of its application to supramolecular materials with desirable photophysical or magnetic properties [8–10], sensors [5, 11, 12], molecular wires [13], mixed-metal supramolecular [8], coordination polymers [14], biochemical and DNA binding properties [15], and supramolecular films [16].

Until now, more than 40 Tppz complexes have been structurally analysed by X-ray diffraction [17], and at least eight kinds of coordination modes have been characterized. These compounds involve mono-, di-, and trinuclear metal complexes in various coordination modes [18–20]. Some of the various coordination modes of Tppz are which illustrate its versatility as a ligand and the possibilities that it offers for the construction of supramolecular metal assemblies [21].

[1] The article is published in the original.

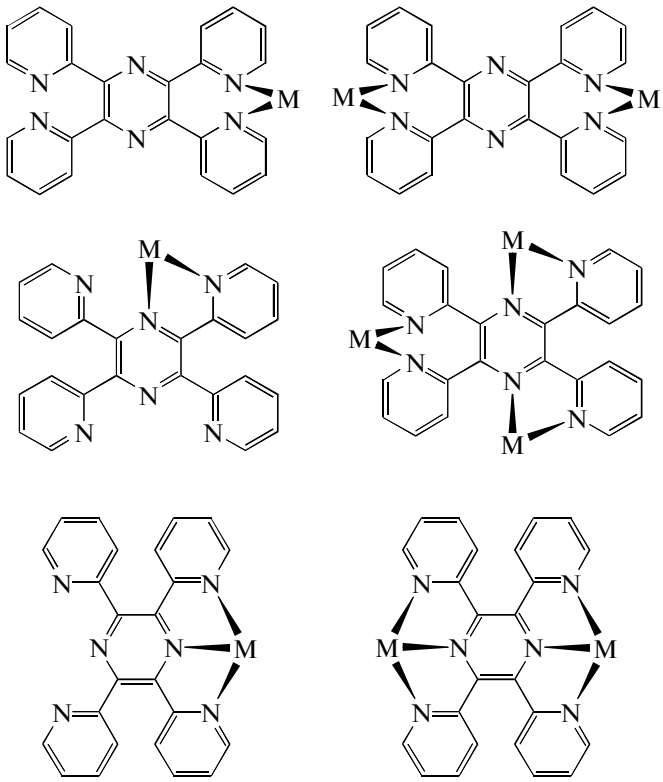

$H_2$Dipic was first discovered in a biological system in 1936 and is now known to be a major component of bacterial spores [22]. $H_2$Dipic is used in a variety of processes as an enzyme inhibitor, plant preservative and food sanitizer [23]. Recent investigations of the $H_2$dipic exhibit that this acid prevents the oxidation of low density lipoprotein, the substance, whose oxidation is involved in the pathogenesis of arteriosclerosis [24]. $H_2$Dipic is a polar aromatic acid that is soluble in organic and chlorinated solvents in the acidic form and thus can penetrate lipid interfaces and be solubilized in hydrophobic environments [25]. $H_2$Dipic has been studied extensively as a Lewis base. $H_2$Dipic and its anions ($HDipic^-$, $Dipic^{2-}$) have proved to be well suited for the construction of multidimensional frameworks, due to the presence of two adjacent O of carboxylate groups as substituents on the *N*-heterocyclic pyridine ring [23, 26]. Among the diversity of dipicolinic acid complexes known, potential applications, in fields of aqueous chemistry, catalysis, biochemistry, as water-soluble drugs, antitumor activity, magnetic materials, in bleaching, bactericidal compositions, development of more effective anti-HIV agents and the design of insulin-mimetic agents [23, 26–29].

It is known that there are a range of different coordination modes with possible monodentate [30], bidentate [31, 32], tridentate [33, 34] or bridging (polymeric, trimeric or dimeric) [35, 36] in transition metal-dipicolinate complexes depending on whether the divalent anionic Dipic ($Dipic^{2-}$), protonated anionic $HDipic^-$ or diprotonated $H_2$Dipic forms are coordinated to metal ions [37].

The work reported in this paper describes the synthesis and characterization of new monomeric and polymeric complexes of Cu(II) and Pb(II) with Tppz ligand, $[Cu(Tppz)(Dipic)] \cdot 8H_2O$ (**I**) and $[Pb_2(Tppz)Cl_4]_n$ (**II**), respectively. At this point in time, the only Tppz-$H_2$Dipic [38] crystal structure reported is that of $[Fe(Tppz)_2][(Dipic)_2Fe]_3 \cdot H_3O \cdot 11H_2O$. The asymmetric unit of $[Fe^{II}(Tppz)_2][Fe^{III}(Dipic)_2]_3 \cdot H_3O \cdot 11H_2O$ contains one $[Fe^{II}(Tppz)_2]^{2+}$ complex, three $[Fe^{III}(Dipic)_2]^-$ counterions, and 12 molecules of water disordered over 23 crystallographic sites. There is no example of crystal structure of mononuclear complex of Tppz-M-Dipic.

## EXPERIMENTAL

**Materials and general methods.** All reagents and solvents used were of reagent grade. Elemental analyses were performed by using a Heraeus CHN-O-Rapid elemental analyzer. FT-IR spectrum was recorded as KBr pellets on FT-IR JASCO 460 spectrophotometer and electronic spectra on a JASCO 7580 spectrophotometer. Cyclic voltammograms were recorded by using a SAMA M-500Research Analyzer.

Three electrodes were utilized in this system, a glassy carbon disk working electrode (diameter 5 mm), a platinum wire auxiliary electrode, and an Ag/AgCl reference electrode. The platinum disk working electrode was manually cleaned with 1-μm diamond polish prior to each scan. The supporting electrolyte, tetrabutylammonium hexafluorophosphate (TBAH), was recrystallized twice from ethanol–water (1 : 1) and vacuum-dried at 110°C overnight. DMSO was distilled over $CaH_2$ and degassed under vacuum prior to use in cyclic voltammetery. The solutions were deoxygenated by bubbling with Ar for 15 min. The procedure performed at room temperature, and Ar atmosphere was maintained over the solution during measurements. Ferrocene ($E° = 0.665$ V versus NHE, $\Delta E_p =$ 60 mV) was used as an internal reference [39]. The range of potentials studied was between +1 and −2.2 V.

**Synthesis of I.** An aqueous solution of copper(II) acetate monohydrate (0.199 g, 1 mmol) (10 mL) and $H_2$Dipic (0.170 g, 1 mmol) in methanol (10 mL) were mixed and stirrered until a blue solution was obtained. The solution was added to a boiling solution of Tppz (100 mg, 1 mmol) in methanol (10 mL). The mixture was stirred for 24 h at 50°C until a green solution was obtained. After 3 days at room temperature, bright green single crystals suitable for X-ray crystallography were formed in a yield of 47%.

| For $C_{31}H_{35}N_7O_{12}Cu$ | | | |
|---|---|---|---|
| anal. calcd., %: | C, 48.92; | H, 4.60; | N, 12.89. |
| Found, %: | C, 48.75; | H, 4.39; | N, 12.71. |

**Synthesis of II.** In a test tube, an acetone (4 mL) solution of $PbCl_2$ (56 mg, 0.2 mmol) was carefully layered on the top of a chloroform (4 mL) solution of Tppz (39 mg, 0.1 mmol) using ethylene glycol (2 mL) as an interlayer. After two weeks at room temperature, bright yellow single crystals suitable for X-ray investigation appeared at the boundary in a yield of 65%.

| For $C_{24}H_{16}N_6Cl_2Pb_2$ | | | |
|---|---|---|---|
| anal. calcd., %: | C, 34.39; | H, 1.91; | N, 10.03. |
| Found, %: | C, 34.45; | H, 1.98; | N, 10.27. |

**X-ray crystallography.** The bright green single crystals of **I** and bright yellow single crystals **II** were grown by the slow evaporation of a 1 : 1 $H_2O$–$C_2H_5OH$ solution of the complex. Single-crystal X-ray diffraction measurements of the complexes were carried out on a Bruker Apex II, using graphite-monochromated Mo$K_\alpha$ radiation ($\lambda = 0.71073$ Å). Unit cell parameters were determined by the least-squares calculations with θ angles ranging from 2.35° to 30.63° for **I** or 2.17° to 28.42° for **II**. The structures were solved by direct and Fourier methods and refined by full-matrix least-squares methods based on $F^2$ using the SHELXS-97 and SHELXL-97 programs [40] giving a final $R_1 =$ 0.0442, $wR_2 = 0.1230$ (for 5960 reflections with $I > 2\sigma(I)$) for **I** and $R_1 = 0.0147$, $wR_2 = 0.0358$ (for 3174 reflections with $I > 2\sigma(I)$) for **II**. All non-hydrogen atoms were readily located and refined using anisotropic thermal parameters. All hydrogen atom positions were refined in the isotropic approximation in a riding model with the $U_{iso}$(H) parameters equal to 1.5 $U_{eq}$(C) for methyl groups and 1.2 $U_{eq}$(C) for other carbon atoms, where $U$(C) are the equivalent thermal parameters of the atoms to which the corresponding H atoms are bonded. The largest diffraction peak and hole on the final difference-Fourier map were 0.557 and −0.431 $e$ Å$^{-3}$ for **I** and 1.097 and −0.959 $e$ Å$^{-3}$ for **II**. Further details of the structural analyses are given in Table 1. The selected bond lengths and angles of complexes **I** and **II** are listed in Table 2. Supplementary material for structures **I**, **II** has been deposited with the Cambridge Crystallographic Data Centre (nos. 874195 (**I**), 874319 (**II**); deposit@ccdc.cam.ac.uk or http://www. ccdc.cam.ac.uk).

## RESULTS AND DISCUSSION

There are three general classes of structures that arise from tridentate-coordination mode of Tppz ligand, including the [M(Tppz)], [M(Tppz)$_2$], and [M$_2$(μ-Tppz)] structures. The simplest of these are the [M(Tppz)] structures that involve coordination of one monotridentate Tppz to a single metal, leaving the other side free [41]. This binding mode is observed for mononuclear Cu(II) complex **I**. Figure 1 shows the coordination geometry of the ligands about the $Cu^{2+}$ ion, that the metal ion $Cu^{2+}$ is six-coordinated by one Tppz and one $H_2$Dipic ligands. The uncoordinated water molecules have been omitted for clarity. Both ligands are tridentate and the coordination sphere around the copper is a distorted octahedral with the N(1)Cu(1)N(3) and O(1)Cu(1)N(2) angles equal to 159.25(9)° and 109.27(8)°, respectively.

The pyridyl rings at the uncoordinated side of the Tppz ligand are planar within experimental errors but the Tppz ligand as a whole is far from being planar due to the steric effects between the hydrogen atoms at the 3-pyridyl positions. Low energy conformations of Tppz are predicted to have each pyridyl ring twisted from coplanarity with the pyrazine by roughly 50° [42–44]. For the coordinated side of the *Tppz* ligand, the dihedral angle between the mean planes of the two coordinated pyridyl rings is 5.92°, whereas that between the two uncoordinated pyridyl rings is 49.98°. It deserves to be noted that the uncoordinated N(5) and N(7) pyridyl nitrogen atoms are slightly shifted up and down from the respective pyrazine ring. Compared with the Cu–N(pyridine) bonds (Cu–N(1) 2.025(2) and Cu–N(3) 2.032(2) Å), the Cu–N(pyrazine) bond (Cu–N(2) 1.950(2) Å) is significantly

**Table 1.** Crystallographic data and structure refinement summary for $[Cu(Tppz)(Dipic)] \cdot 8H_2O$ (**I**) and $[Pb_2(Tppz)Cl_4]_n$ (**II**)

| Parameter | Value | |
|---|---|---|
| | **I** | **II** |
| Formula weight | 761.20 | 472.31 |
| Temperature, K | 293(2) | 150(2) |
| Crystal system | Monoclinic | Triclinic |
| Space group | $C2/c$ | $P\bar{1}$ |
| $a$, Å | 35.421(3) | 7.9534(4) |
| $b$, Å | 8.422(6) | 8.8682(5) |
| $c$, Å | 22.824(8) | 9.4245(5) |
| α, deg | 90 | 93.422(2) |
| β, deg | 101.69(2) | 95.086(2) |
| γ, deg | 90 | 96.707(2) |
| $V$, Å$^3$ | 6668(5) | 655.93(6) |
| $Z$ | 8 | 2 |
| $\rho_{calcd}$, mg/m$^3$ | 1.517 | 2.391 |
| Crystal size, mm | 0.48 × 0.23 × 0.22 | 0.23 × 0.22 × 0.04 |
| Range of $h$, $k$, $l$ | $-43 \le h \le 43$, $-10 \le k \le 10$, $-28 \le l \le 28$ | $-10 \le h \le 10$, $-11 \le k \le 11$, $-12 \le l \le 12$ |
| $F$(000) | 3064.0 | 434.0 |
| θ Ranges, deg | 2.35–30.63 | 2.17–28.42 |
| Reflections collected | 109810 | 10641 |
| Independent reflections ($R_{int}$) | 6546 (0.0410) | 3255 (0.0248) |
| Data/restraints/parameters | 6546/5/481 | 3174/0/163 |
| Goodness-of-fit on $F^2$ | 1.061 | 1.051 |
| Final $R$ indices | $R_1 = 0.0442$, $wR_2 = 0.1230$ | $R_1 = 0.0147$, $wR_2 = 0.0358$ |
| $R$ indices (all data) | $R_1 = 0.0490$, $wR_2 = 0.1311$ | $R_1 = 0.0151$, $wR_2 = 0.0359$ |

shorter. This behavior is probably caused by the stronger π-accepting properties of the pyrazine ring.

Also in the complex **I**, the $Cu^{2+}$ ion is coordinated by the tridentate $H_2$Dipic ligand through the two oxygen atoms of two carboxylate groups and nitrogen atom of pyridine ring. Two carboxylate oxygen atoms (O(1) and O(2)) from $Dipic^{2-}$ and two nitrogen atoms (N(1) and N(3)) of the pyridine rings of the Tppz ligand comprise the equatorial plane while nitrogen atoms of $Dipic^{2-}$ ligand N(4) and nitrogen atom N(2) of the pyrazine ring of the Tppz ligand occupy the axial positions. All the solvate water molecules and all the carboxylate oxygens of the Dipic ligand are involved in hydrogen bonding, which cause the stability of the crystal structure (Fig. 2).

The complex **II** is a neutral and polymeric complex in which the Tppz ligand in a bis-tridentate coordination mode together with chlorine atoms function in bridging manner to link divalent lead ions and to form two-dimensional polymeric structure (Fig. 3). The structure of **II** contains a $PbN_3Cl_4$ sphere with a coordination number of seven. One crystallographically distinct lead atom is chelated by one side of Tppz ligand with three heterocyclic nitrogen atoms of pyridyl and pyrazine moieties (Pb(1)–N(1) 2.6210(19), Pb(1)–N(8) 2.8556(19), and Pb(1)–

**Table 2.** Selected bond lengths (Å) and angles (deg) for **I** and **II***

| Bond | *d*, Å | Bond | *d*, Å |
|---|---|---|---|
| **I** | | **II** | |
| Cu(1)–N(1) | 2.025(2) | Pb(1)–Cl(1) | 2.8141(6) |
| Cu(1)–N(2) | 1.950(2) | Pb(1)–Cl(2) | 3.0579(6) |
| Cu(1)–N(3) | 2.032(2) | Pb(1)–N(1) | 2.6210(19) |
| Cu(1)–N(4) | 1.997(2) | Pb(1)–N(8) | 2.8556(19) |
| Cu(1)–O(1) | 2.357(2) | Pb(1)–N(11) | 2.953(2) |
| Cu(1)–O(2) | 2.291(2) | Pb(1)–Cl(2)$^{i}$ | 2.7697(7) |
| | | Pb(1)–Cl(1)$^{ii}$ | 2.9890(7) |
| Angle | ω, deg | Angle | ω, deg |
| **I** | | **II** | |
| N(2)Cu(1)N(4) | 175.62(8) | Cl(1)Pb(1)Cl(2) | 88.98(2) |
| N(2)Cu(1)N(1) | 79.66(8) | Cl(1)Pb(1)N(1) | 81.91(4) |
| N(4)Cu(1)N(1) | 98.34(8) | Cl(1)Pb(1)N(8) | 134.35(5) |
| N(2)Cu(1)N(3) | 79.67(8) | Cl(1)Pb(1)N(11) | 162.53(5) |
| N(4)Cu(1)N(3) | 102.40(8) | Cl(1)Pb(1)Cl(2)$^{i}$ | 91.67(2) |
| N(1)Cu(1)N(3) | 159.25(9) | Cl(1)Pb(1)Cl(1)$^{ii}$ | 79.92(2) |
| N(2)Cu(1)O(2) | 99.92(8) | Cl(2)Pb(1)N(1) | 158.80(5) |
| N(4)Cu(1)O(2) | 76.19(8) | Cl(2)Pb(1)N(8) | 135.65(4) |
| N(1)Cu(1)O(2) | 92.06(8) | Cl(2)Pb(1)N(11) | 77.97(5) |
| N(3)Cu(1)O(2) | 93.21(8) | Cl(2)Pb(1)Cl(2)$^{i}$ | 81.12(2) |
| N(4)Cu(1)O(1) | 74.66(8) | N(1) Pb(1)N(8) | 58.98(6) |
| N(1)Cu(1)O(1) | 93.90(8) | Cl(2)$^{i}$Pb(1)N(1) | 80.07(5) |
| N(3)Cu(1)O(1) | 91.23(8) | Cl(1)$^{ii}$Pb(1) N(1) | 81.01(5) |
| O(2)Cu(1)O(1) | 150.80(7) | Cl(2)$^{i}$Pb(1)N(8) | 102.69(4) |
| | | Cl(1)$^{ii}$Pb(1) N(8) | 72.07(5) |
| | | Cl(1)$^{ii}$Pb(1)Cl(2)$^{i}$ | 160.20(2) |

* Symmetry codes: $^{i}$ $-x, -y, -z$, $^{ii}$ $1-x, -y, -z$.

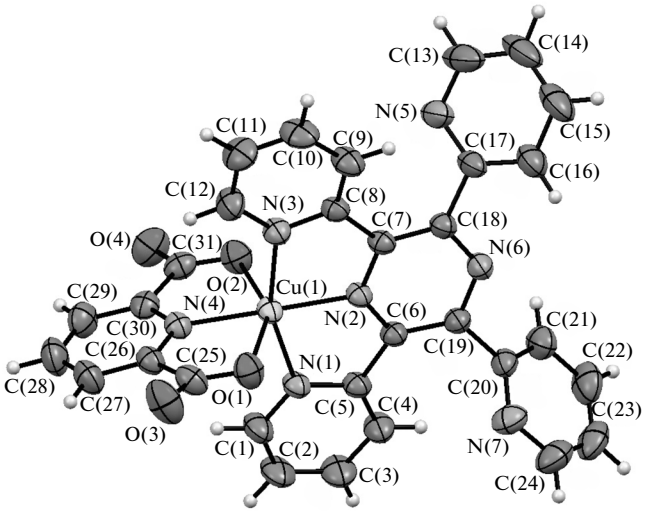


**Fig. 1.** View of the coordination environment of the Cu(II) in **I**. The uncoordinated water molecules have been omitted for clarity.

N(11) 2.953(2) Å) and is coordinated by four chlorine atoms (Pb(1)–Cl(1) 2.8141(6), Pb(1)–Cl(2) 3.0579(6), Pb(1)–Cl(1)$^{ii}$ 2.9890(7), and Pb(1)–Cl(2)$^{i}$ 2.7697(7) Å) (symmetry codes: $^{i}$ $-x, -y, -z$, $^{ii}$ $1-x, -y, -z$). The N(8)Pb(1)N(1) and N(8)Pb(1)N(11) angles equal to 58.98(6)° and 57.68(6)°, respectively, indicated to the constraints imposed by 5-memberd chelate ring of Tppz ligand (Fig. 4).

The chelation of Tppz ligand to Pb occurs in such a way that the planarity of ligand is distorted by the rotation of pyridyl rings with respect to pyrazine ring. The angle between best planes of pyridyl and pyrazine rings, which are 32.33° and 48.18° for each pyridyl moiety, indicated that pyridyl rings is tilted from pyrazine ring to gain the adaptable direction in the coordination manner. A remarkable feature in the molecular structure of complex **I** was the presence of Tppz ligand as a bridging moiety between $[PbCl_2]_n$ polymeric chains which resulted in two-dimensional polymeric structure. In addition, the crystal structure analysis reveals that the molecular sheets of complex **I** involved the hydrogen-bonded interactions from the bridging Cl atoms of one layer to the C atoms from pyridyl rings in a neighboring layer, which are C–H···Cl non-classical hydrogen bonds (C(4)···Cl(1) 3.682, C(4)–H(4*A*)···Cl(1) 2.896 Å and C(3)···Cl(2) 3.649 Å, C(3)–H(3*A*)···Cl(2) 2.865 Å) (Fig. 5). So the complex **I** can be described as an extended three-dimensional supramolecular structure via intermolecular non-classical hydrogen bonds.

Data for the infrared spectra for Tppz, $H_2$Dipic, and complex were obtained as solid in KBr. Predominant vibrations for the free Tppz ligand are associated with ν(C=C), ν(C=N), and ring stretching. The reported separation between ν(C=C) and ν(C=N) is closed to 20 $cm^{-1}$ for polypyridyl ligands [45, 46], and thus the observed vibrational absorption bands for Tppz at 1592 and 1567 $cm^{-1}$ may be due to either different ν(C=N) on the pyrazine and pyridine rings or ν(C=C) and ν(C=N) with coincidental equivalence of the different rings [46]. An intense band at 1393 $cm^{-1}$ is assigned to ring stretching of both pyrazine and pyridine rings of Tppz. The FT–IR spectrum of **I** shows a absorption pattern in 4000–400 $cm^{-1}$ region similar to Dipic and Tppz ligands.

The FT–IR bands of **I** were assigned by comparing with the free Tppz values. This complex shows moderately sharp absorptions at 1595, 1572, and 1395 $cm^{-1}$ which is assigned to the stretching of coordinated Tppz ligand. In both compounds, OH vibration of water molecules gives broad bands at 3400–3600 $cm^{-1}$. The broadness of this band indicates the presence of hydrogen bonds involving water molecules in both complexes [45]. In all the complexes, the band due to $\nu_{as}(COO^{-})$ was observed in the region 1675–

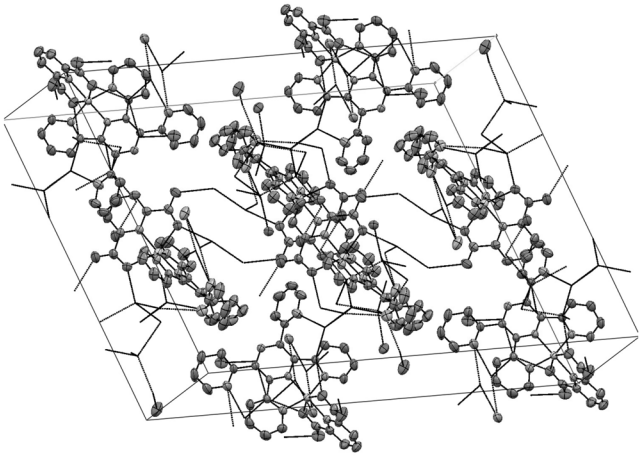

**Fig. 2.** Fragment of crystal packing (projection along *y* crystal axis) of **I**. The hydrogen atoms uncoordinated water molecules have been omitted for clarity.

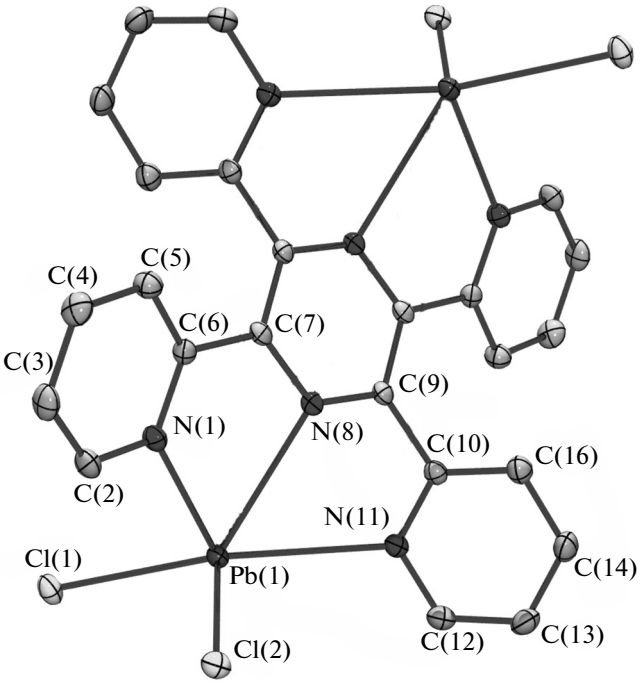


**Fig. 3.** The structure of **II** showing displacement ellipsoids at the 50% probability level. Unlabeled atoms are related to label atoms by the symmetry code $-x, -y, -z$. The hydrgen atoms have been omitted for clarity.

1610 $cm^{-1}$ and that due to $\nu_s(COO^-)$ in the region 1352–1344 $cm^{-1}$. A large difference of 327–307 $cm^{-1}$ between $\nu_{as}$ and $\nu_s$ vibrations indicates a monodentate coordination of the carboxylic group in all the complexes [47]. The asymmetric and symmetric stretching bands of the carboxylate group $\nu_{as}(COO^-)$ are observed at 1640 and 1473 $cm^{-1}$, respectively, for **I**. An intense band at 1393 $cm^{-1}$ is assigned to ring stretching of both the pyrazine and pyridine rings of Tppz. The FT–IR bands of **II** were assigned by comparing with the free Tppz values. Infrared spectra in KBr displayed bands corresponding to ν(C=N) at ~1594 $cm^{-1}$ and bands around 286–332 $cm^{-1}$ assignable to ν(M–Cl). These values compare well with the reported FT–IR bands in the Tppz complexes [45].

The electronic absorption spectroscopy of **I** was found to be quite complicated due to the many possible transitions. It is possible to have Tppz $\pi \rightarrow \pi^*$ and $n \rightarrow \pi^*$ transitions as well as ligand field (**LF**) ($t_{2g}^6 \rightarrow e_g^3$), MLCT (Cu → Tppz and/or Cu → Dipic) transitions [48]. Absorption spectrum of complexes **I** and **II** in DMSO displayed band at 268 and 245 nm, respectively.

Cyclic voltammetry was performed on an acetonitrile solution of **I** with 0.1 M TBAH as a supporting electrolyte (Fig. 6). The CV of $H_2$Dipic shows two overlapping irreversible reduction peaks at −1.36 and −1.56 V which do not display associated oxidation processes in the reverse scan, even at the highest scan rate [49]. It should be mentioned that the electrochemical behavior of **I** is characterized by metal based and ligand based reductions. The first irreversible two-electron reduction (−0.77 V) is assigned as Cu(II/I), the second and third reductions (−1.11 and −1.46 V) are assigned as $Tppz^{0/-}$ and $Tppz^{-/-2}$. The Dipic ligand shows an irreversible behavior at −1.62 V. The $Tppz^{0/-}$ and $Tppz^{-/-2}$ couples occur prior to the dipic due to the larger π system of Tppz ligand as a result of the two

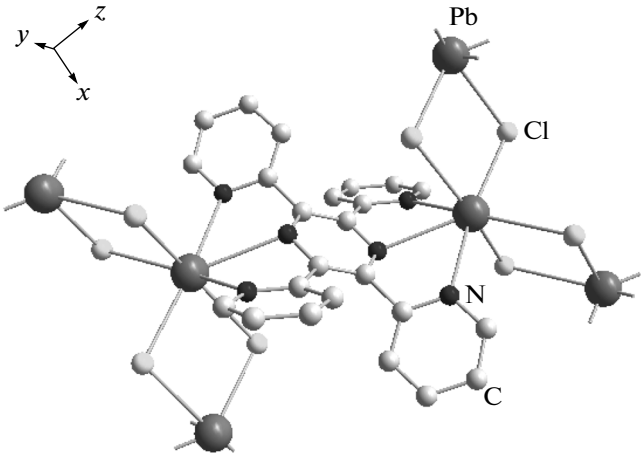


**Fig. 4.** A representation of coordination environment of divalent lead atom in complex **II**.

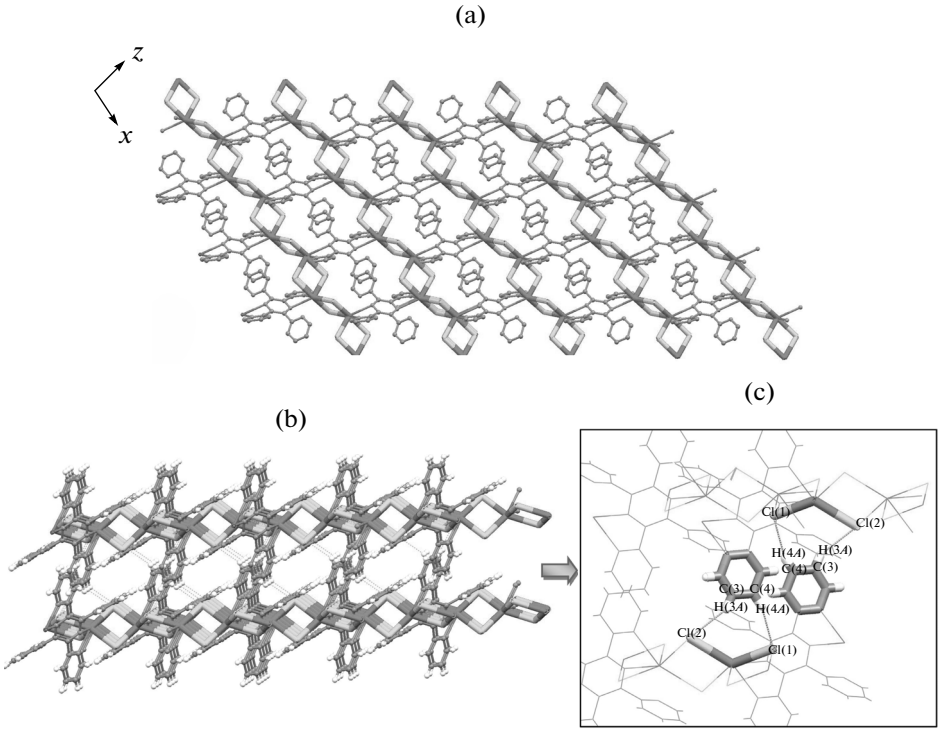


**Fig. 5.** A representation of crystal packing of complex **II** in *y* direction (a); C–H···Cl interactions between layers of polymeric structure are presented as dotted orange lines in side view (b); some parts of the packing together labels of C–H···Cl interactions are represented in wire-frame mode for clarity (c).

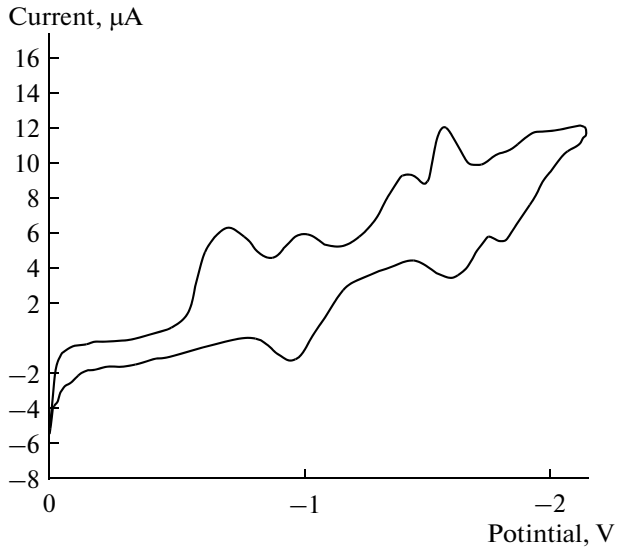


**Fig. 6.** Cyclic voltammogram of **I** in DMSO at scan rate of 100 mV $s^{-1}$; 0.1 M TBAH as a supporting electrolyte.

extra pyridyl rings on Tppz as well as the extra electron accepting character of the pyrazine ring [50].

## REFERENCES

1. Gibson, V.C., Redshaw, C., and Solan, G.A., *Chem. Rev.*, 2007, vol. 107, p. 1745.
2. Balzani, V., Juris, A., Venturi, M., et al., *Chem. Rev.*, 1996, vol. 96, p. 759.
3. Newkome, G.R., He, E., and Moorefield, C.N., *Chem. Rev.*, 1999, vol. 99, p. 1689.
4. Danks, J.P., Champness, N.R., and Schröder, M., *Coord. Chem. Rev.,* 1998, vol. 174, p. 417.

5. Alves, W.A., Fiorito, P.A., Córdoba de Torresi, S.I., and Torresi, R.M., *Biosen. Bioelectron.*, 2006, vol. 22, p. 298.
6. Trivedi, M., Pandey, D.S., and Rath, N.P., *Inorg. Chim. Acta*, 2009, vol. 362 p, p. 284.
7. Goodwin, H.A. and Lions, F., *J. Am. Chem. Soc.*, 1959, vol. 81, p. 6415.
8. Carranza, J., Brennan, C., Sletten, J., et al., *Inorg. Chem.*, 2003, vol. 42, p. 8716.
9. Burkholder, E., Wright, S., Golub, V., et al., *Inorg. Chem.*, 2003, vol. 42, p. 7460.
10. Burkholder, E., Golub, V., O'Connor, C.J., and Zubieta, J., *Inorg. Chem.*, 2004, vol. 43, p. 7014.
11. Maskus, M. and Abruña, H.D., *Langmuir*, 1996, vol. 12, p. 4455.
12. Yuasa, J. and Fukuzumi, S., *J. Am. Chem. Soc.*, 2008, vol. 130, p. 566.
13. Flores-Torres, S., Hutchison, G.R., Soltzberg, L.J., and Abruña, H.D., *J. Am. Chem. Soc.*, 2006, vol. 128, p. 1513.
14. Fantacci, S., De Angelis, F., Wang, J., et al., *J. Am. Chem. Soc.*, 2004, vol. 126, p. 9715.
15. Rubino, S., Portanova, P., Girasolo, A., et al., *Eur. J. Med. Chem.*, 2009, vol. 44, p. 1041.
16. Alves, W.A., Pfaffen, V., Ortiz, P.I.S.I., et al., *J. Braz. Chem. Soc.*, 2008, vol. 19, p. 651.
17. Allen, F.H., *Acta Crystallogr., Sect. B: Struct. Sci.*, 2002, vol. 58, p. 380.
18. Maekawa, M., Minematsu, T., Konaka, H., et al., *Inorg. Chim. Acta*, 2004, vol. 357, p. 3456.
19. Sadjadi, M.S., Ebadi, A., Zare, K., et al., *Acta Crystallogr., Sect E: Structure Reports Online*, 2008, vol. 64, p. 1050.
20. Teles, W.M., Speziali, N.L., and Filgueiras, C.A.L., *Polyhedron*, 2000, vol. 19, p. 739.
21. Padgett, C.W., Pennington, W.T., and Hanks, T.W., *Cryst. Growth. Des.*, 2005, vol. 5, p. 737.
22. Xie, J.R.H., Smith, V.H., Jr., and Allen, R.E., *Chem. Phys.*, 2006, vol. 322, p. 254.
23. Kirillova, M.V., Da Silva, M.F.C.G., Kirillov, A.M., et al., *Inorg. Chim. Acta*, 2007, vol. 360, p. 506.
24. Vargova, Z., Zeleoak, V., Cisaova, I., and Gyoryova, K., *Thermochim. Acta*, 2004, vol. 423, p. 149.
25. Crans, D.C., Trujillo, A.M., Bonetti, S., et al., *J. Org. Chem.*, 2008, vol. 73, p. 9633.
26. Park, H., Lough, A.J., Kim, J.C., et al., *Inorg. Chim. Acta*, 2007, vol. 360, p. 2819.
27. Szorcsik, A., Nagy, L., Deak, A., et al., *J. Org. Chem.*, 2004, vol. 689, p. 2762.
28. Ucar, I., Karabulut, B., Bulut, A., and Buyukgungor, O., *J. Mol. Struct.*, 2007, vol. 336, p. 834.
29. Moghimi, A., Moosavi, S.M., Kordestani, D., et al., *J. Mol. Struct.,* 2007, vol. 828, p. 38.
30. Gourdon, P.L.A. and Launay, J.P., *Inorg. Chem.*, 1995, vol. 34, p. 5129.
31. Buglyó, P., Crans, D.C., Nagy, E.M., et al., *Inorg. Chem.*, 2005, vol. 44, p. 416.
32. Wang, Y., Odoko, M., and Okabe, N., *Acta Crystallogr., Sect. E: Found. Crystallogr.*, 2004, vol. 60, p. 1178.
33. Okabe, N. and Oya, N., *Acta Crystallogr., Sect. C: Cryst. Struct. Commun.*, 2000, vol. 56, p. 305.
34. Perry, J.J., McManus, G.J., and Zaworotko, M.J., *J. Chem. Crystallogr.*, 2004, vol. 34, p. 877.
35. Du, M., Cai, H., and Zhao, X.J., *Inorg. Chim. Acta*, 2006, vol. 359, p. 673.
36. Gourdon, P.L.A. and Launay, J.P., *Inorg. Chem.*, 1995, vol. 34, p. 5138.
37. Drew, M.G.B., Fowles, G.W.A., Matthews, R.W., and Walton, R.A., *J. Am. Chem. Soc.*, 1969, vol. 9, p. 7769.
38. Lainé, P., Gourdon, A., and Launay, J.P., *Inorg. Chem.*, 1995, vol. 34, p. 5156.
39. Gennett, T., Milner, D.F., and Weaver, M.J., *J. Phys. Chem.*, 1985, vol. 89, p. 2787.
40. Sheldrick, G.M., *SHELXS-97, a Program for Crystal Structure Solution and SHELXL-97, a Program for Crystal Structure Refinement*, Göttingen (Germany): Univ. of Göttingen, 2008.
41. Padgett, C.W., Pennington, W.T., and Hanks, T.W., *Cryst. Growth. Des.*, 2005, vol. 5, p. 737.
42. Flores-Torres, S., Hutchison, G.R., Soltzberg, L.J., and Abruna, H.D., *J. Am. Chem. Soc.*, 2006, vol. 128, p. 1513.
43. Fantacci, S., de Angelis, F., Wang, J., et al., *J. Am. Chem. Soc.*, 2004, vol. 126, p. 9715.
44. Rubino, S., Portanova, P., Girasolo, A., et al., *Eur. J. Med. Chem.*, 2009, vol. 44, p. 1041.
45. Nakamato, K., *Infrared and Raman Spectra of Inorganic and Coordination Compounds*, New York: Wiley, 2009.
46. Ruminski, R.R. and Letner, C., *Inorg. Chim. Acta*, 1989, vol. 162, p. 175.
47. Baro, A.C.G., Castellano, E.E., Piro, O.E., and Costa, B.S.P., *Polyhedron*, 2005, vol. 24, p. 49.
48. Lever, A.B.P., *Inorganic Electronic Spectroscopy*, Amsterdam: Elsevier, 1984.
49. González-Baró, A.C., Pis-Diez, R., Piro, O.E., and Parajón-Costa, B.S., *Polyhedron*, 2008, vol. 27, p. 502.
50. Saljooghi, A.Sh. and Fatemi, S.J.A., *Russ. J. Coord. Chem.*, 2011, vol. 37, p. 168.